Interannual Variability of Phytoplankton Abundances in the North Atlantic.

Stephanie Dutkiewicz*, Mick Follows and John Marshall

Department of Earth, Atmospheric and Planetary Sciences
Massachusetts Institute of Technology
54-1511, 77 Massachusetts Ave
Cambridge, MA 02139

Watson W. Gregg

NASA Goddard Space Flight Center
Laboratory for Hydrospheric Processes
Greenbelt, MD 20771

Deep-Sea Research: accepted for publication (January 2000)

* Corresponding author: e-mail, stephd@plume.mit.edu; phone, 617-253-6430; fax, 617-253-4464

ABSTRACT

A framework is developed for examining spatial patterns of interannual variability in spring-time chlorophyll concentrations as a response to physical changes. A simplified, two-layer bio-physical model reveals regional responses to interannual variability of convective mixing. Vertical mixing can promote productivity in the surface waters through enhanced nutrient supply, but can also retard productivity due to the transport of phytoplankton below Sverdrup's critical depth. The balance of these processes determines the regimes of response in the two-layer model. The regimes may be identified by the ratio of the thickness of Sverdrup's critical layer during spring and the end of winter mixed layer, h_c/h_m.

The responses predicted by the simplified model are found in a more sophisticated four-compartment, nitrogen based ecosystem model, driven by a general circulation model of the North Atlantic. Anomalously strong convective mixing leads to enhanced chlorophyll concentrations in regions of shallow mixed layers ($h_c/h_m \sim 1$), such as the subtropics. In contrast, in the subpolar regions where mixed layers are deeper ($h_c/h_m \ll 1$), the sensitivity to convective mixing is weaker, and increased mixing can lead to lower phytoplankton abundances. The numerical model also reveals regions of more complex behavior, such as the inter-gyre boundary, where advective supply of nutrients plays a significant role on interannual timescales.

Preliminary analyses of *in situ* and remote observations from the Bermuda Atlantic Time-Series, Ocean Weather Station "India" and the Coastal Zone Color Scanner also show qualitative agreement. The conceptual framework provides a tool for the analysis of ongoing remote ocean color observations.

1 Introduction

Long term, *in situ* time series observations show significant interannual variability in surface nutrient and chlorophyll concentrations. For example, data sets collected between 1990 and 1996 at the Bermuda Atlantic Time Series (BATS) site in the subtropical gyre show that springtime nutrient and chlorophyll concentrations increase with convective mixing (Michaels and Knap, 1996). In contrast, investigations by Stramska et al (1995) of chlorophyll and mixing events close to OWS "India", in the subpolar gyre, show that a strong mixing event in the spring of 1991 was associated with lower chlorophyll concentrations than in 1989 when the waters were more stratified. Several studies have suggested that local plankton variability is related to changes in regional climate and patterns of meteorological forcing: Aebischer et al (1990), Frommentin and Planque (1998), Taylor and Stephens (1980), Reid et al (1998) have described the variability found in the Continuous Plankton Recorder (CPR) Data in the Northern North-East Atlantic and North Sea. Correlations are found between plankton variability and indicators of local weather and climate shifts, such as the North Atlantic Oscillation and the position of the north wall of the Gulf Stream.

Observations, then, suggest that there are complex relationships between physical and biological patterns which appear to be different in physically distinct regions. In this manuscript we develop a framework within which we can begin to address the question: How do regional patterns of interannual variability in chlorophyll distributions reflect the variability in the underlying physical environment?

We investigate the interplay between physical and biological dynamics and their respective roles in setting and modulating spatial and interannual variability of the springtime chlorophyll signal. In Section 2, we develop a simple two-layer model to study the interplay of nutrient cycling and vertical mixing in controlling springtime phytoplankton concentrations. We identify a non-dimensional parameter, h_c/h_m – the ratio of the local critical depth [1], h_c and end of winter mixed layer depth, h_m – which characterizes regional regimes

[1] "Critical depth" in this study is defined as the depth above which, in the absence of nutrient limitation, there would be a net growth in phytoplankton.

of the spring chlorophyll response to interannual variability in springtime mixing activity. In Section 3 we describe a more complex three-dimensional North Atlantic biogeochemical model, and in section 4 the interannual variability of chlorophyll in this three-dimensional biogeochemical model is shown to behave broadly as predicted by the two-layer model. In Section 5, using remote and *in situ* observations, we briefly illustrate the application of this conceptual tool to the analysis of observed data.

2 A Two-layer Light and Nutrient Limited Ecological Model

On seasonal time scales it is generally reasonable to assume that nutrient supply to the euphotic zone is controlled primarily by vertical processes, such as convective mixing and vertical advection (e.g. Steele and Henderson, 1993; Williams and Follows, 1998). Wintertime convective mixing sets the available nutrients for new production and interannual variations of winter convection may modulate springtime productivity.

The subsequent onset of the spring bloom in the North Atlantic is, in part, a consequence of the re-stratification of the water column following relatively deep winter mixing. Re-stratification, however, is not instantaneous, and may be an intermittent process punctuated by the passage of synoptic weather systems as illustrated schematically in Fig. 1 (see, for example, Stramska et al, 1995). Anomalous vertical mixing during the spring may enhance chlorophyll concentrations through continued nutrient supply. Conversely, phytoplankton growth may become (or continue to be) light limited, with metabolic processes outweighing net growth within the mixed layer, as identified by the Sverdrup (1953) "critical depth" theory. What is the effect of this competition of light and nutrients on the interannual variation of spring surface chlorophyll? To describe the interplay between the supply of nutrients by convection and the availability of light during the spring bloom, we formulate a highly idealized, two layer physical-ecological model, depicted schematically in Fig. 2. The system, a tool for exploration, contains the essential ingredients: nutrient and light limited growth of phytoplankton, mortality and grazing, and active vertical mixing within the seasonal boundary layer. Two layers represent the end of winter mixed layer (h_m): the depth to which intermittent mixing might occur. The upper layer is the critical layer (as

defined in the previous section), h_c, with phytoplankton abundance, P, and macro-nutrient concentration, N. The remainder of the mixed layer $(h_m - h_c)$ is disphotic. We describe the system as follows:

$$\begin{aligned}
\frac{dN}{dt} &= -\mu\frac{N}{(N+N_o)}P + \kappa(1-\frac{h_c}{h_m})(N_T - N) \\
\frac{dP}{dt} &= +\mu\frac{N}{(N+N_o)}P - \beta P - \kappa(1-\frac{h_c}{h_m})P \\
N_T &= constant \\
P_T &= 0. \qquad (1)
\end{aligned}$$

The growth of plankton is described by a Michaelis-Menton parameterization, with half-saturation nutrient concentration of N_o and a maximum growth rate of μ. Losses due to metabolism and grazing are represented simply as βP (where β is the loss rate), and are assumed to not be re-available for biological production during the springtime. Zooplankton and dissolved organic matter are not explicitly represented. Growth rate μ is held constant for mean spring-time conditions. The lower layer nutrient concentration (N_T) is fixed assuming a relatively large reservoir, and phytoplankton concentration (P_T) is zero, assuming that mortality and grazing strongly dominate. Vertically averaged, mean spring-time mixing within the seasonal boundary layer is represented by the rate constant κ, and its influence is scaled by the relative thickness of the layers $(1 - h_c/h_m)$.

Our focus here is on the influence of interannual variability of spring mixing which is, in turn, induced by interannual variability in air-sea interactions. We investigate the sensitivity of spring-time phytoplankton to the physical parameters κ and h_c/h_m by integrating the equations (1) over the spring period in appropriate ranges of h_c/h_m and κ. We initialize the integration with reasonable values of N and P for end of winter conditions and plausible choices of μ, N_o, N_T and β.

Figure 3 shows the springtime (two month) average nutrient and phytoplankton concentrations normalized by N_T for several of these integrations. (We examined the sensitivity to initial conditions and integration period and find that the results depicted are qualitatively robust when other reasonable initial conditions and parameters are used.) We depict curves for two regimes of h_c/h_m, (subtropical $h_c/h_m \sim 0.8$; and subpolar, $h_c/h_m \sim 0.2$), and

highlight solutions in parameter space appropriate for those regimes. The figure shows that more active mixing always increases the nutrient concentration in the critical layer (Fig. 3a) but anomalously increased mixing may lead to increased or decreased phytoplankton concentrations, and this behavior is governed by the ratio of the critical depth to the mixed layer depth and vigor of the mixing.

In the subtropical regime, where h_c/h_m is close to 1 and mixing rates are usually relatively low, an increase in mixing enhances the phytoplankton concentration by supplying increased nutrients to the upper layer (solid line in Fig. 3b). In the subpolar regime, however, the mixed layer depth can be considerably deeper than the critical depth such that with sufficient turbulent mixing within the boundary layer, $(1 - h_c/h_m)\kappa$ is large. In such regions, springtime mixing may still be vigorous (Stramska et al, 1995). According to this simple model, and as illustrated by the dashed curve in Figure 3(b), at low mixing rates plankton concentrations will increase, but at higher rates (more typical of the subpolar region) phytoplankton concentrations diminish with enhanced mixing. In the latter case, plankton are mixed to depths where there is insufficient light for growth. With high mixing rates though, the dashed curve suggests that phytoplankton concentrations become lower and are increasingly less sensitive to the enhanced mixing. Concentrations will be higher in years of weaker mixing because the phytoplankton spend more time growing in the euphotic zone.

For very high mixing in low h_c/h_m regions (i.e. dashed curve in Fig. 3b), the strong negative gradient in P/N_T weakens. A scale analysis of Equation 1 suggests an approximate e-folding timescale for the development of P where h_c/h_m is small; $\tau = 1/(\mu - \beta - \kappa)$. For relatively weak mixing, μ is large compared to $(\beta + \kappa)$ and this timescale is on the order of days; the mean of the springtime transient solution approaches the long term steady-state solution. However, as $(\beta + \kappa)$ approaches μ (stronger mixing), P evolves relatively slowly. Here, the timescale to approach steady state is much longer than the spring period, the springtime average of P does not approach the long term steady state, and the sensitivity of P/N_T to κ is weaker. At very high mixing rates in these low h_c/h_m regions $(\beta + \kappa \geq \mu)$, net growth cannot occur: $P/N_T = 0$, and $d(P/N_T)/d\kappa = 0$.

This model expresses the key elements of Sverdrup's (1953) critical depth theory in a form that can address interannual variability of spring-time mixing. Because it makes specific predictions about regional trends in phytoplankton variability as a function of changes in mixing rates and availability of light, it provides a simple framework from which to contemplate observations and more complex models. However, because the model neglects much of the complexity required to accurately represent marine ecosystems, we now present a more detailed physical and ecological model of the North Atlantic and examine its interannual variability from the perspective provided by this simplified model.

3 A Model of Interannual Ecosystem Variability in the North Atlantic

We combine a four compartment nitrogen based ecosystem and a North Atlantic circulation model with time-varying forcing. The individual components of the model are discussed in this section.

3.1 Ecosystem Model

The ecosystem model represents the flow of nitrogen between four compartments: inorganic nitrogen (N), phytoplankton (P), zooplankton (Z) and dissolved organic matter (D). Such compartmental ecosystem models have long been used in studies of marine ecology (e.g. Riley, 1947; Steele, 1958) and been successfully applied in ecosystem studies on the scale of ocean gyres (Fasham et al, 1993; Sarmiento et al, 1993; McCreary et al, 1996). Nitrogen is thought to be the limiting nutrient for many oceanic communities, and is therefore often used as a primary variable (Fasham et al, 1990; Doney et al, 1996; McGillicuddy et al, 1995; Marra and Ho, 1993). The model can be written as (symbols are defined in Table 1):

$$\begin{aligned}
\frac{dN}{dt} &= -\mu_o \frac{I}{(I+I_o)} \frac{N}{(N+N_o)} P + e_p P + e_z Z + rD + F \\
\frac{dP}{dt} &= +\mu_o \frac{I}{(I+I_o)} \frac{N}{(N+N_o)} P - e_p P - m_p P - g \frac{P}{(P+P_o)} Z \\
\frac{dZ}{dt} &= +g \frac{P}{(P+P_o)} Z - e_z Z - m_{z2} Z^2
\end{aligned}$$

$$\frac{dD}{dt} = +d(m_p P + m_{z2} Z^2) - rD. \quad (2)$$

were $\frac{d}{dt}$ represents the time rate of change following the motion of a fluid parcel. The phytoplankton growth rate is determined by the availability of light and nutrients (inorganic nitrogen, N). The Michaelis-Menton form is used to parameterize, separately, the effect of nutrient concentration on nutrient uptake ($N/(N+N_o)$) and light availability on photosynthetic rate ($I/(I+I_o)$). The effect of both on the growth rate of phytoplankton is multiplicative. Metabolism of phytoplankton consists of excretions (e_p), which return nitrogen to the inorganic pool, and mortality (m_p). A fraction, d, of the mortality term becomes nitrogen in a semi-labile pool of dissolved organic matter (D) that is remineralized to an inorganic form within weeks. The remainder, $(1-d)$, is sinking particulate material which is assumed to instantly remineralize to an inorganic form at depth. The flux of PON from each layer is assumed to have an exponential profile, similar to that suggested by Najjar et al (1992). This flux F at model level k is described as:

$$F = \sum_{n=1}^{k-1} (1-d)(m_p P_n + m_{z2} Z_n^2) e^{\frac{(h(n)-h(k))}{h_o}}$$

where $h(n)$ is the depth of the n-th level. Phytoplankton are grazed (g) by zooplankton, Z, at a rate parameterized by a Michaelis-Menton scheme. A quadratic mortality factor for zooplankton (m_{z2}) is chosen to include effects of internal grazing in the zooplankton pool. Such a quadratic form also provides a more stable ecosystem than a linear term (Steele and Henderson, 1992; Broström and Drange, 1999).

The values of the ecosystem model parameters (Table 1) are constrained by oceanic observations and laboratory studies where these are available. Otherwise, the parameter choices are within the range employed in similar models (Fasham et al, 1990; Marra and Ho, 1993; Doney et al, 1996; McGillicuddy et al, 1995). Sensitivity to the parameter values was examined through a suite of experiments in which individual parameter values were changed. It is sufficient to state here that, although some features of the mean fields are sensitive to the parameter choices, the conclusions we draw in this paper with regard to interannual variability are not compromised, provided that plausible parameters are chosen.

3.2 Light Model

Surface irradiance with 25nm spectral resolution required for phytoplankton growth are computed using detailed radiative transfer analyses which include the effects of atmospheric optical constituents. Monthly climatologies of atmospheric pressure, wind speed, relative humidity, and precipitable water were obtained from the NOAA Surface Marine Atlas (da Silva et al, 1994), ozone from the Total Ozone Mapping Spectrometer for 1983-1990 from the Goddard Space Flight Center Distributed Active Archive Center (GSFC-DAAC; Greenbelt, MD), and cloud information was obtained from the International Satellite Cloud Climatology Project (ISCCP, from the GSFC-DAAC) also for the years 1983-1990. Under clear conditions, surface irradiance are computed as a function of climatological pressure, wind speed, relative humidity, precipitable water, and ozone according to Gregg and Carder (1990). When cloudy, cloud optical thickness and liquid water path information from ISCCP are used to compute low spectral surface irradiance using the model of Slingo (1989). Spectral (350 – 700 nm) irradiance with 25nm resolution just below the surface of the water are thus specified for each degree area in the North Atlantic. Monthly climatologies from this period are applied in the North Atlantic model. Light is attenuated through the water column by coefficients for water molecules K_w, phytoplankton $k_c C$ and colored dissolved organic matter K_g following Gregg and Walsh (1992):

$$K_d(\lambda, h) = K_w(\lambda) + \sum_{n=1}^{k} (k_c(\lambda))_n C_n + K_g(\lambda)$$

where λ is wavelength, C_n is the chlorophyll concentration in a grid cell at level n using a phytoplankton nitrogen/chlorophyll ratio of 1.59 μM (mg m^{-3})$^{-1}$ as suggested by Fasham et al (1990). The spectral seawater and chlorophyll-specific absorption and total scattering coefficients were derived from Baker and Smith (1982). The total light available for growth, I, in each model grid cell is computed from the spectral irradiance at each depth.

3.3 Ocean Circulation and Tracer Transport

We use the MIT ocean general circulation model described in Marshall et al (1997) and Marshall et al (1999) in a global configuration at $1^\circ \times 1^\circ$ resolution, with realistic geometry

and topography. There are 21 levels, whose thickness ranged from 25 m in the surface euphotic zone to 500 m near the ocean bottom. The model was forced by twice-daily NCEP analyzed wind stresses and daily NCEP heat fluxes (Kalnay et al, 1996) for the years 1987 to 1995. The model adopts a transformed Eulerian mean representation of tracer transport (following Gent and McWilliams, 1990) and a simple representation of convection as described by Marshall and Schott (1999). The monthly-mean circulation fields are stored and used in an "off-line" model to transport the biogeochemical tracers (*i.e.* N, P, Z, D) of the ecosystem model in the North Atlantic sector. For arbitrary tracer, A:

$$\frac{\partial A}{\partial t} = -\nabla \cdot (\vec{u^*} A) + \nabla \cdot (\mathbf{K} \nabla A) + J + C.$$

Biogeochemical variables are advected by the transformed Eulerian mean circulation, $\vec{u^*}$. Eddy stirring is constrained to act along isopycnals through the mixing tensor $\mathbf{K}$. The advection scheme is 3rd order upwind and a time-step of 3 hours is used. The term J represents the biological sources and sinks, discussed in Section 3.1, and C represents the vertical mixing due to convection. Convective mixing is parameterized in the off-line model by allowing vertically adjacent grid cells to homogenize tracer concentrations as frequently as statically unstable conditions were found in those columns of grid cells in the "on-line" model.

Figure 4 shows the model 1992 spring sea surface temperature and the associated geostrophic streamfunction. The model reproduces the large scale features of the region, with subpolar and subtropical gyres separated by the North Atlantic Current, the seaward extension of the Gulf Stream. The simplified model in Section 2 indicated the importance of the depth of winter convective mixing and the vigor of convective mixing into the spring period; it is therefore important that the general circulation model has a plausible distribution of mixed-layer depths. In Figure 5 we show comparisons of mixed-layer depths diagnosed from the model subtropical and subpolar regions (see Fig. 4), and from BATS and OWS "India" observations. The model produces the magnitude and timing of the re-stratification of the water column relatively well. Mixed-layer depth and convective mixing activity are closely related to surface fluxes of heat. For example the anomaly of the surface sensible heat flux (Fig. 6), used as part of the forcing, does have similar patterns as the anomaly of

the model convective mixing (Fig. 7).

The offline model domain is initialized with an inorganic nitrogen concentration corresponding to the nitrate climatology from Conkright et al (1994). Nitrogen in phytoplankton and zooplankton are initialized as a fraction of the inorganic values. The model domain is the North Atlantic from -5^{o}N to 80 ^{o}N and 110^{o}W to 22^{o}E. Tracer concentrations near open boundaries are restored towards initial conditions on a short timescale. Since biological activity is for the most part limited to the upper few hundred meters in the open ocean, inorganic nitrogen concentrations are restored towards climatology below 1000 m, and the organic components are set to zero there. The model was run for 150 years, driven by repeatedly cycling through the 9 year sequence of physical fields.

4 Variability in Modeled Nutrient and Chlorophyll Distributions

Our aim is to capture gross features of the regional variations and the annual cycle in the North Atlantic with the simplest viable representation of the highly complex ecosystem. In later sections we examine and characterize the response of modeled phytoplankton abundances to interannual variability in the physical environment. But can the model reproduce the broad characteristics of the North Atlantic chlorophyll distribution? We begin by comparing the model's "climatological" distribution and seasonal cycle of chlorophyll with those inferred from remote and *in situ* observations.

4.1 Mean Seasonal Cycle: Comparison to Observations

Figure 8 shows with solid lines the monthly averaged (for the 9 years) chlorophyll concentrations in the upper 25 m of the model for the three regions - "subpolar", "intergyre" and "subtropical" (regions depicted in Fig. 4). The area-averaged chlorophyll concentrations from monthly composites of 1998 SeaWiFS (Sea-viewing Wide Field-of-view Sensor) data for the same regions are shown for comparison. The broad pattern of low phytoplankton biomass in the subtropics and seasonally high biomass in the subpolar regions is captured by the model. The model also captures the seasonal cycles and seasonal peak amplitudes. However, given that some potentially important processes are neglected such as nitrogen

fixation, explicit geostrophic eddies, multiple phytoplankton species, micro-nutrient limitation and a constant Chl:N ratio is assumed, the model cannot be expected to perform uniformly well over the entire model domain. In the subtropics the spring seasonal peak of modeled chlorophyll appears slightly later than in the one year of SeaWiFS data measurements, but within the envelope of peak months observed in *in situ* BATS data (also shown). There is also a tendency for plankton abundances to become too low during the summer and fall months. However *in situ* measurements at BATS (Michaels and Knap, 1996) do show similarly low values as our model in summer months (dotted line in Fig. 8). Oschlies and Garçon (1998) have found that inclusion of transfer on the scale of geostrophic eddies improves the fidelity of ecosystem models particularly in the subtropical gyre, a process that is only represented parametrically in our model. In general, though, our model does capture the large-scale spatial and temporal variability seen in satellite data, suggesting that it is a useful "laboratory" in which to study mechanisms of interannual variability in the nutrients and chlorophyll concentrations.

4.2 Interannual Variability

4.2.1 One-dimensional Perspective

Spring Nutrients

Nutrient concentrations are in most areas strongly related to the strength of local convective mixing. Figure 7 and Figure 9 show the spring/winter anomaly of convective mixing and inorganic nitrogen concentration in the upper 50 m for years 1989 and 1991. Anomalously weak convection over the subtropics in 1989 has corresponding lower nutrient concentrations, while higher than normal nutrients and convective mixing are found for the same year in the northern portion of the model domain. In Figure 10(a) we examine the model's inorganic nitrogen behavior in the framework suggested by the idealized two-layer model of Section 2: the model spring inorganic nitrogen concentration averaged over the upper 50 m, normalized by winter nutrients, are plotted against spring convective mixing rates, determined from model convective mixing statistics. Variability in mixing rates is a consequence of variability in the spring forcing in each of the 9 years. For each region a symbol indi-

cates the individual spring-average mixing rate and the mean spring normalized inorganic nitrogen concentration. We find that increased mixing will enhance available nutrients at the surface in all regions, in accord with the predictions of the simplified model of Section 2, shown in Fig. 3 (a).

Spring Phytoplankton

The two-layer model of Section 2 suggests that the underlying mechanisms of interannual plankton variability are more complicated than that of nutrient supply. Phytoplankton variability is affected by both nutrient and light limitation. We identified an important non-dimensional parameter, h_c/h_m – the ratio of the local critical depth, h_c and end of winter mixed layer depth, h_m – which characterizes regional regimes of the spring chlorophyll response to interannual variability in mixing activity. The regional variation of the model's 9 year mean h_c/h_m ratio is shown in Figure 11. Here h_c is taken as the springtime critical depth – the depth to which model net phytoplankton growth (with no nutrient limitation) is greater than the loss due to excretion and mortality ($\sum_{k=1}^{h_c} \mu_o \frac{I}{(I+I_o)} P_k = \sum_{k=1}^{h_c} (e_p + m_p) P_k$, see Eqn. 2). The end of winter mixed layer depth, h_m, is defined as the depth where the difference between the temperature at depth and the sea-surface temperature is greater than 0.5^oC. We find that the subtropics are characterized by high values of this ratio, while subpolar regions have much lower values. The three regions of Figure 4 have different h_c/h_m ratios: about 0.8 in the subtropics, 0.4 in the intergyre region and about 0.2 in the subpolar region. We expect these regions to exhibit different trends in chlorophyll concentrations as mixing rates vary from year to year.

The seasonal cycle of phytoplankton abundance is largely controlled by the availability of nutrients (either supplied from below or laterally by currents) and of sunlight (from above). In this model the growth rate of plankton is determined by the multiplicative effect of both these processes. Figure 12 plots, as suggested by Equation 2, $I/(I + I_o)$ and $N/(N + N_o)$, and their product averaged over the top 50 m of each region for three consecutive years. The growth rate is limited more by light in the two northern regions of the model (where h_c/h_m is low) than in the subtropics (where h_c/h_m is close to 1). In subpolar regions nutrients may be stirred (or advected) to the upper layers, but it is only when sufficient

sunlight becomes available that significant growth occurs. Moreover, convective mixing in the subpolar regions occurs to greater depths than the subtropics because the stratification is weaker and the forcing stronger (hence the smaller h_c/h_m ratios). Figure 10(b) shows the normalized spring phytoplankton concentration averaged over the upper 50 m of the model. There is clearly an increase in spring phytoplankton concentrations (relative to the available nutrients) with enhanced springtime mixing in the subtropical region (compare to the solid curve in Figure 3b). An increase in the mixing brings additional nutrients to the growing region and thereby increases plankton concentrations. However, for greater mixed layer depths (smaller h_c/h_m ratios), the competition between the extra supply of nutrients and the length of time phytoplankton spend in the critical layer becomes more crucial. If mixing rates are enhanced markedly, the phytoplankton concentrations decrease even though nutrient concentrations increase. The trends in the mean springtime values in the subpolar region of the model can be compared to the low h_c/h_m curve (dashed) in Figure 3(b). The regional differences in the effect of spring mixing on phytoplankton abundance variability in this more complex bio-physical model, is as predicted by the two-layer model of Section 2. However, the numerical model results shown in Figure 10 do show more scatter than predicted by the one-dimensional model, suggesting that the there are other factors beyond this one-dimensional perspective that can affect interannual variability.

4.2.2 Intergyre Region and the Role of Advection

The simple model developed above predicts particular behavior in regions of extreme h_c/h_m according to a simple one dimensional view. In the intergyre region, however, intermediate h_c/h_m renders this view limited in its usefulness, confirmed by Fig. 10 where there is no clear trend in the intergyre variability. In this region warm, nutrient poor water from the Gulf Stream meets with colder, nutrient rich water from the Labrador Current. The diagnostic study of Williams and Follows (1998) demonstrates that this region is also subject to strong advective influence on nutrient supply.

Figure 13(a) shows the modeled monthly inorganic nitrogen profile for year 1987 to 1995 in the intergyre region. The higher than normal winter nutrient signal in 1991 and 1992

cannot be explained by increased convective mixing (Fig. 7). During these years there is also colder water in the region than in preceding years (Fig. 13 b), suggesting that the region is dominated by a different water mass during this period. In our model there is an enhanced influx of inorganic nitrogen into the region beginning in 1990 as indicated by the increasingly positive flux observed in all but the winter months in Figure 13(c). Figure 13(d) shows the meridional transport of inorganic nitrogen (in mol/s) in the top 100 m of the model Labrador Current across 51^oN (transect shown in Fig. 4). The increased supply to the intergyre region corresponds to the increased southward transport of inorganic nitrogen out of the Labrador Sea by the current. Interannual variability in the strength of the Labrador Current and its inorganic nitrogen concentration will therefore affect nutrient concentrations in the intergyre region. The simple local balance described in Section 2 is insufficient to describe this region.

5 Discussion and Comparison with Observations

We have employed a simple two layer ecosystem model to isolate the effects of changes in boundary layer mixing rates on phytoplankton abundances. Regimes are identified in terms of the non-dimensional parameter h_c/h_m, the ratio of the thickness of the spring critical layer depth to the end of winter mixed layer depth. We find that for realistic levels of mixing:

• In regions where h_c/h_m is relatively large (such as the subtropics) anomalously high spring mixing leads to enhanced chlorophyll

• In regions where h_c/h_m is relatively small (such as the subpolar gyre) anomalously high spring mixing decreases surface chlorophyll concentrations, although the response is weaker.

The theory is borne out in a more complex three-dimensional physical-biological model of the North Atlantic, with a four compartment, nitrogen based ecosystem model. This model is able to reproduce the gross regional and seasonal distributions of chlorophyll in the North Atlantic. When forced with interannually varying meteorological fields, we find that the qualitative response in chlorophyll of this more complex model is broadly consistent with

that predicted by the simplified two-layer model.

These results must be interpreted within the limitations of the ecosystem and physical models adopted. The physical model has a coarse resolution in both the horizontal and the vertical. In the subtropics in particular, eddies may be crucial for the supply of nutrients to the surface layers in non-winter months (McGillicuddy et al, 1998; Oschlies and Garçon, 1998) and nitrogen fixation may be a significant source of new nitrogen (Michaels et al, 1996). The ecosystem model is necessarily simple, employing the minimum number of nitrogen compartments and parameters to resolve the first order signal of plankton abundances. We view the two-layer and numerical models as a laboratory for the development and testing of ideas about a complex system, rather than as a simulation tool.

We have used the h_c/h_m ratio to identify broad regions in the North Atlantic ocean where the biological response to changes in large scale physical forcing may be expected to be qualitatively different. The Bermuda Atlantic Time-Series Station falls in a regime where climatologically h_c/h_m is close to 1. We would expect a positive response in chlorophyll to enhanced spring mixing. Plotting spring time chlorophyll against NCEP surface heat loss (as a proxy for mixing activity) in Figure 14 (a), we do indeed find a clear positive correlation, showing good qualitative agreement with both the two-layer model and the North Atlantic model in as much as the heat flux reflects mixing rates. Ocean Weather Station "India" is in the subpolar gyre where the h_c/h_m ratio is smaller, typically less than 0.25. Our models predict a negative relationship between high spring mixing and chlorophyll concentrations in this regime. Data from the weather station are, however, inconclusive (see Fig. 14 b): the observational record at OWS "I" is too short to draw any firm conclusions.

Remote observations can give significantly better spatial and temporal resolution. Images from the Coastal Zone Color Scanner (CZCS) show interannual differences over large areas in the surface concentrations of chlorophyll in the North Atlantic. Since the sensor shared the satellite platform with several other instruments, it was not operating at all times: the images may therefore give a distorted view of the variability. Given this caveat, we consider data from 7 years (1979 to 1985) of the CZCS data. We calculate mean spring chlorophyll concentrations for bins that compare to the three regions shown in Figure 4.

In Figure 15(a) we plot these springtime average chlorophyll concentrations against NCEP analyzed mean surface sensible heat flux for the years with sufficient color data. We can see suggestions of a positive correlation between increasing heat flux (one mechanism indicative of convective mixing) and chlorophyll concentrations in the subtropical region and a negative trend in the subpolar region. As expected, there is a more ambiguous signal in the intergyre region. Figure 15(b) shows model results averaged to 50 m for these regions. The CZCS trends follow our expectations from both our simple and more complex models, suggesting that a more detailed study using SeaWiFS data and more sophisticated interpretation of heat fluxes in terms of mixing rates will be instructive. The data demands a closer, more mechanistic interpretation of relationships between physical and biological parameters. Such a study is the focus of future work.

In summary, we have considered a mechanistically based examination of the springtime biological response to physical forcing. The interannual variability of nutrient supply and phytoplankton abundances have been investigated in a simple two layer construct and in a more complex numerical model in order to identify regional patterns of response to interannual variability in the boundary layer mixing. We also examine remote and *in situ* observed time series of chlorophyll in this novel way, and find the simple framework provides a consistent and useful diagnostic tool. We plan to use these concepts to interpret causes of variability in the ongoing Sea-viewing Wide Field-of-view Sensor (SeaWiFS), and forthcoming Moderate Resolution Imaging Spectroradiometer (MODIS), data sets.

ACKNOWLEDGEMENTS

The authors thank Chris Hill and Alistair Adcroft for their contribution to the development of both the MITgcm and the off-line model, and Detlef Stammer for providing the model fields used in this study. The numerical experiments described here were carried out on an SMP cluster called "Pleiades" – donated by Digital Corporation and housed at MIT's Laboratory for Computer Science. SeaWiFS and CZCS data used by the authors was provided by the Earth Observing System Data and Information System (EOSDIS), Distributed Active Archive Center at Goddard Space Flight Center. The authors also used data from the Bermuda Atlantic Time-series Station (BATS) and Hydrostation S programs that were funded by grants from the National Science Foundation to the Bermuda Biological Station for Research, Inc., and data from Ocean Weather Station "India" kindly provided by the PRIME program. Comments from Dave Siegel and two anonymous reviewers have helped to clarify the ideas expressed in this paper. This study is funded by a grant from NASA (number NCC5-244).

References

Aebischer, N.J., J.C. Coulson and J.M. Colebrook, 1990. Parallel long-term trends across four marine trophic levels and weather. *Nature* 347, 753 – 755.

Archer, D., E.T. Peltzer and D.L. Kichman, 1997. A timescale for dissolved organic carbon production in equatorial Pacific surface waters. *Global Biogeochemical Cycles* 11, 435 – 452.

Baker, K.S. and R.C. Smith, 1982. Bio-optical classification and model of natural water. 2. *Limnology and Oceanography* 27, 500 – 509.

Broström, G. and H. Drange, 1999. On the mathematical formulation of the marine plankton system. *Sarsia*, submitted.

Conkright, M., S. Levitus, and T. Boyer, 1994. *World Ocean Atlas 1994 Volume 1: Nutrients.* NOAA Atlas NESDIS 1, U.S. Department of Commerce, Washington, D.C.

da Silva, A.M., C.C. Young, and S. Levitus, 1994. *Atlas of surface marine data 1994 Volume 1: algorithms and procedures.* NOAA Atlas NESDIS 6, U.S. Department of Commerce, Washington, D.C., 83 pp.

Doney, S.C., D.M. Glover and R.G. Najjar, 1996. A new coupled, one-dimensional biological-physical model for the upper ocean: Applications to the JGOFS Bermuda Atlantic time series (BATS) site. *Deep-Sea Research* 43, 591 – 624.

Eppley, R.W., 1972. Temperature and phytoplankton growth in the sea. *Fishery Bulletin* 70, 1,063 – 1,085.

Eppley, R.W. and E.M. Renger, 1974. Nitrogen assimilation of an oceanic diatom in nitrogen-limited continuous culture. *Journal of Phycology* 18, 534 – 551.

Fasham, M.J.R., H.W. Ducklow and S.M. McKelvie, 1990. A nitrogen-based model of plankton dynamics in the oceanic mixed layer. *Journal of Marine Research* 48, 591 – 639.

Fasham, M.J.R., J.L. Sarmiento, R.D. Slater, H.W. Ducklow and R. Williams, 1993. A seasonal three-dimensional ecosystem model of nitrogen cycling in the North Atlantic euphotic zone: A comparison of the model results with observations from Bermuda Station "S" and OWS "India". *Global Biogeochemical Cycles* 7, 379 – 415.

Frommentin, J.M. and B. Planque, 1998. North Atlantic oscillation and year-to-year plankton fluctuations. http://www.npm.ac.uk/sahfos/staff/nao.html.

Gent, P. and J. McWilliams, 1990. Isopycnal mixing in ocean circulation models. *Journal of Physical Oceanography* 20, 150 – 155.

Gregg, W.W. and J.J. Walsh, 1992. Simulation of the 1979 spring bloom in the Mid-Atlantic Bight: A coupled physical/biological/optical model. *Journal of Geophysical Research* 97, 5,723 – 5,743.

Gregg, W.W. and K.L. Carder, 1990. A simple spectral solar irradiance model for cloudless maritime atmospheres. *Limnology and Oceanography* 35, 1,657 – 1,675.

Hansell, D.A. and T.Y. Waterhouse, 1997. Controls on the distributions of organic carbon and nitrogen in the eastern Pacific Ocean. *Deep-Sea Research* 44, 843 – 857.

Kalney, E., M. Kanamitsu, R. Kistler, W. Collins, D. Deaven, L. Gandin, M.M. Chelliah, W. Ebisuzaki, W. Higgins, J. Janowiak, K.C. Mo, C. Ropelewski, J. Wang, R. Jenne and D. Joseph, 1996. The NCEP/NCAR 40-year reanalysis project. *Bulletin of the American Meteorological Society* 77, 437 – 472.

Lohrenz, S.E., G.A. Knauer, V.L. Asper, M. Tuel, M. Michaels and A.F. Knap, 1992. Seasonal variability in primary production and particle flux in the northwestern Sargasso Sea: U.S. JGOFS Bermuda Atlantic Time-series Study. *Deep-Sea Research* 39, 1,373 – 1,391.

Marra, J. and C. Ho, 1993. Initiation of the spring bloom in the northeast Atlantic (47^oN, 20^oW): A numerical simulation. *Deep-Sea Research* 40, 55 – 73.

Marshall, J.C. and F. Schott, 1999. Open-ocean convection: Observations, theory and models. *Reviews of Geophysics* 37, 1 – 64.

Marshall, J.C., C. Hill, L. Perelman and A. Adcroft, 1997. Hydrostatic, quasi-hydrostatic and non-hydrostatic ocean modeling. *Journal of Geophysical Research* 102, 5,733 – 5,752.

Marshall, J., D. Jamous and J. Nilsson, 1999. Reconciling "thermodynamic" and "dynamic" methods of computation of water-mass transformation rates. *Deep-Sea Research*, 46, 545 – 572.

Martin, J.H., G.A. Knauer, D.M. Karl and W.W. Broenkow, 1987. VERTEX: Carbon cycling in the northeastern Pacific. *Deep-Sea Research* 34, 267 – 285.

McCreary, J.P., K.E. Kohler, R.R. Hood and D.B. Olson, 1996. A four-component ecosystem model of biological activity in the Arabian Sea. *Progress in Oceanography* 37, 193 – 240.

McGillicuddy, D.J., A.R. Robinson, D.A. Siegal, H.W. Jannasch, R. Johnson, T.D. Dickey, J. McNeil, A.F. Michaels and A.H. Knap, 1998. Influence of mesoscale eddies on new production in the Sargasso Sea. *Nature* 394, 263 – 266.

McGillicuddy, D.J., J.J. McCarthy and A.R. Robinson, 1995. Coupled physical and biological modeling of the spring bloom in the North Atlantic (I): Model formulation and one dimensional bloom processes. *Deep-Sea Research* 42, 1,313 – 1357.

Michaels, A.F. and A.H. Knap, 1996. Overview of the U.S. JGOFS Bermuda Atlantic time-series study and Hydrostation "S" program. *Deep-Sea Research* 43, 157 –198.

Michaels, A.F., D. Olson, J.L Sarmiento, J.W. Ammerman, K. Fanning, R. Jahnke, A.H. Knap, F. Lipschultz and J.M. Prospero, 1996. Inputs, losses and transformations of nitrogen and phosphorus in the pelagic North Atlantic.
In Howarth, R.W. (Ed.), *Nitrogen Cycling in the North Atlantic Ocean and Its Watersheds*, Kluwer Academic Publishers, Boston, MA, pp. 181-226.

Najjar, R.G., J.L. Sarmiento and J.R. Toggweiler, 1992. Downward transport and fate of organic matter in the ocean: Simulations with a general circulation model. *Global Biogeochemical Cycles* 6, 45 – 76.

Oschlies, A. and V. Garçon, 1998. Eddy-induced enhancement of primary production in a model of the North Atlantic ocean. *Nature* 394, 266 – 269.

Parson, T.R., M. Takahashi and B. Hargrave, 1990. *Biological Oceanogrpahic Processes.* Pergamon Press, Oxford U.K., 330pp.

Reid, P.C., M. Edwards, H.G. Hunt and A.J. Warner, 1998. Phytoplankton change in the North Atlantic. *Nature* 391, .

Rhee, G-Y and I.J. Gotham, 1981. The effect of enviromental factors on the phytoplankton growth: Light and the interactions of light with nitrate limitation. *Limnology and*

Oceanography 26, 649 – 659.

Riley, G.A., 1947. A theoretical analysis of the zooplankton population of Georges Bank. *Journal of Marine Research* 6, 104 – 113.

Sakshaug, E. and D. Slagstad, 1991. Light and productivity of phytoplankton in polar marine ecosystems: a physiological view. *Polar Research* 10, 579 – 591.

Sarmiento, J.L., R.D. Slater, M.J.R. Fasham, H.W. Ducklow, J.R. Toggeweiler and G.T. Evans, 1993. A seasonal three-dimensional ecosystem model of nitrogen cycling in the North Atlantic euphotic zone. *Global Biogeochemical Cycles* 7, 417 – 450.

Slingo, A., 1989. A GCM parameterization for the shortwave radiative properties of water clouds. *Journal of Atmospheric Sciences* 46, 1,419 – 1,427.

Steele, J.H., 1958. Plant production in the northern North Sea. Scottish Home Department, Marine Research report 7. HMSO, Edinburgh.

Steele, J.H. and E.W. Henderson, 1992. The role of predation in plankton models. *Journal of Plankton Research* 14, 157 – 172.

Stramska, M, T.D. Dickey, A. Plueddemann, R. Weller, C. Langdon and J. Marra, 1995. Bio-optical variability associated with phytoplankton dynamics in the North Atlantic ocean during spring and summer of 1991. *Journal of Geophysical Research* 100, 6,621 – 6,632.

Sverdrup, H.U., 1953. On conditions of the vernal blooming of phytoplankton. *Journal du conseil international pour l'exploration de la mer* 18, 287 – 295.

Taylor, A.H. and J.A. Stephens, 1980. Latitudinal displacement of the Gulf Stream (1966 to 1977) and their relation to changes in temperature and zooplankton abundances in the NE Atlantic. *Oceanology Acta* 3, 145 – 149.

Williams, R.G. and M.J. Follows, 1998. The Ekman transfer of nutrients and maintenance of new production over the North Atlantic. *Deep-Sea Research* 45, 461 – 489.

Yamanaka, Y. and E. Tajika, 1997. The role of dissolved organic matter in the marine biogeochemical cycle: Studies using and ocean biogeochemical general circulation model. *Global Biogeochemical Cycles* 11, 599.

List of Figures

inorganic nitrogen	N		μ M
nitrogen in phytoplankton	P		μ M
nitrogen in zooplankton	Z		μ M
dissolved organic nitrogen	D		μ M
available light	I		W m^{-2}
particle flux	F		μ M d^{-1}
phytoplankton maximum growth rate	μ_o	1/0.6	d^{-1}
half saturation light intensity	I_o	30	W m^{-2}
half saturation inorganic nitrogen	N_o	0.1	μ M
phytoplankton excretion rate	e_p	1/20	d^{-1}
zooplankton excretion rate	e_z	1/30	d^{-1}
DON remineralization rate	r	1/45	d^{-1}
phytoplankton mortality rate	m_p	1/10	d^{-1}
zooplankton grazing rate	g	1/1.6	d^{-1}
half saturation phytoplankton	P_o	0.9	μ M
zooplankton quadratic mortality rate	m_{z2}	0.2	(μ M d)$^{-1}$
fraction PON becoming DON	d	0.5	
e-folding fallout depth	h_o	400	m

Table 1: **Symbols and Parameters of Ecosystem Model.** Estimates of maximum phytoplankton growth rates (μ_o) lie between $\frac{1}{2}$ and 4 d^{-1} (Eppley, 1972; Eppley and Renger, 1974). The half-saturation light constant (I_o) varies between species of phytoplankton and has been measured to range from 5 to 100 W/m^2 (Parson et al, 1990; Sakshaug and Slagstad, 1991; Rhee and Gotham, 1981). The half saturation of nitrate uptake also varies with species, but we choose .1 μM as more representative of oceanic species (Eppley and Renger, 1974). Phytoplankton excretion and mortality rates are difficult to determine experimentally. Fasham et al (1990) used phytoplankton mortality as a free parameter in their model and found values of $\frac{1}{11}$ d^{-1} appeared to give the best results. Zooplankton grazing rate, plankton half saturation values and zooplankton excretion rates are also suggested by a combination of observations and previous ecosystem models (e.g. Riley, 1947; Fasham et al, 1990). The quadratic zooplankton mortality value was chosen following Steele and Henderson (1992) and Broström and Drange (1999). Recent observations (Hansell and Waterhouse, 1997) suggest that a significant fraction (about half) of net community production forms "semi-labile" DOM. Modeling studies suggest that the remineralization rate of this DOM is of order weeks to months (e.g. Archer et al, 1997; Yamanaka and Tajika, 1997). Values of the particulate remineralization scale length (h_o) are suggested by sediment trap measurements (Lohrenz et al, 1992; Martin et al, 1987).

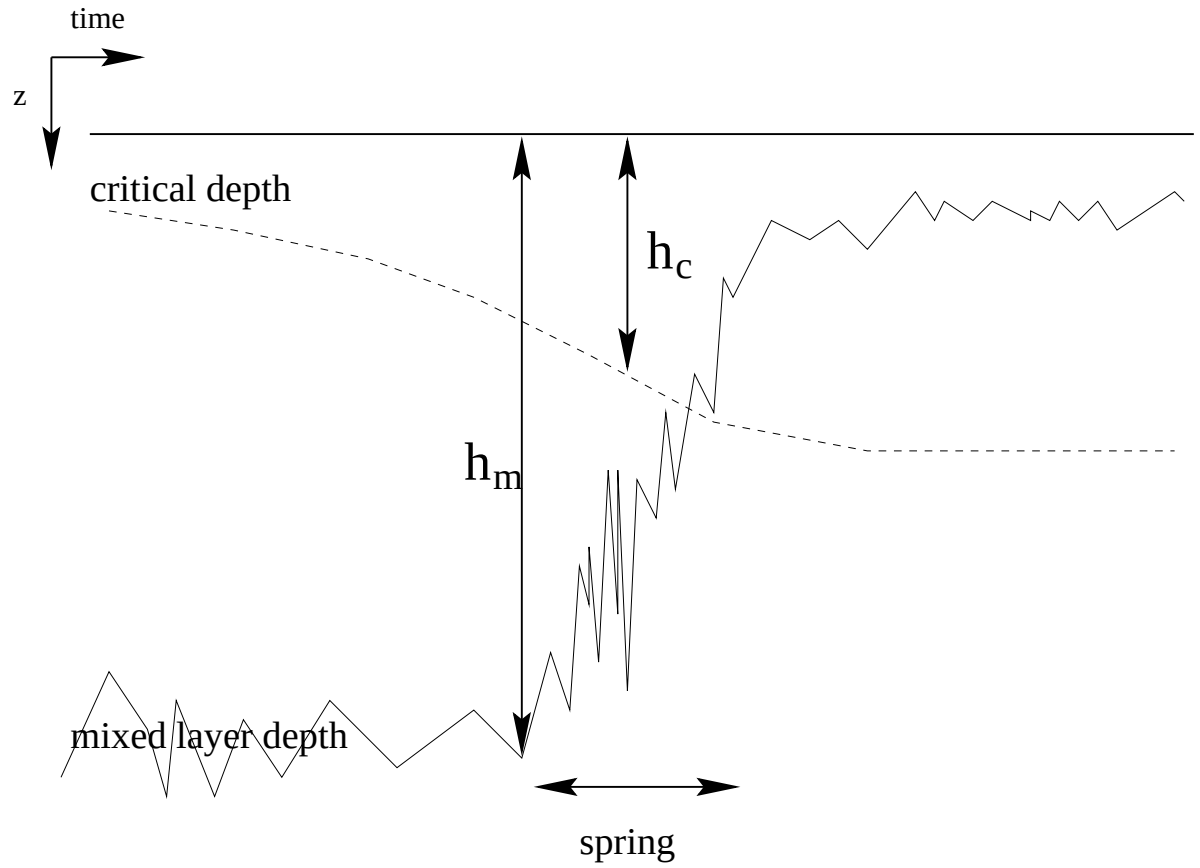

Figure 1: Schematic of mixed layer depth (solid line) and critical depth (dashed line) from mid winter to summer. The spring period of interest to this study (i.e. timing of the onset of the spring bloom) is indicated.

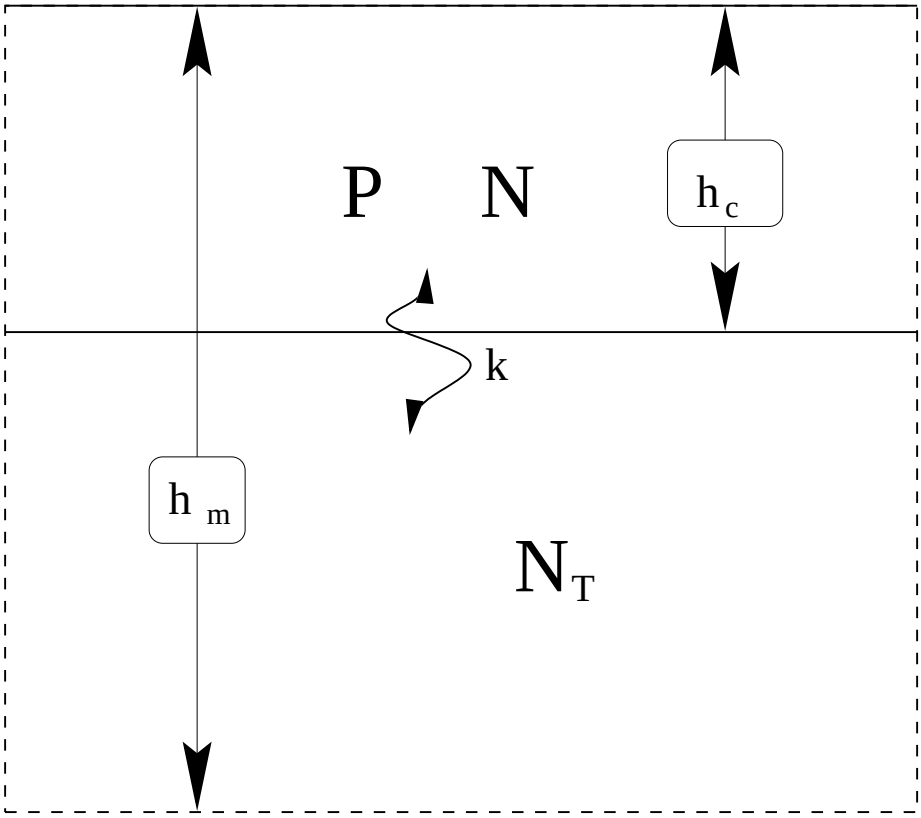

Figure 2: Schematic of two layer system used in Equation 1, representing the end of winter mixed layer h_m separated into the critical layer h_c and the disphotic portion of the mixed layer. P and N denote upper layer phytoplankton and nutrient concentrations respectively; N_T is the lower layer nutrient concentrations; κ is the mixing coefficient.

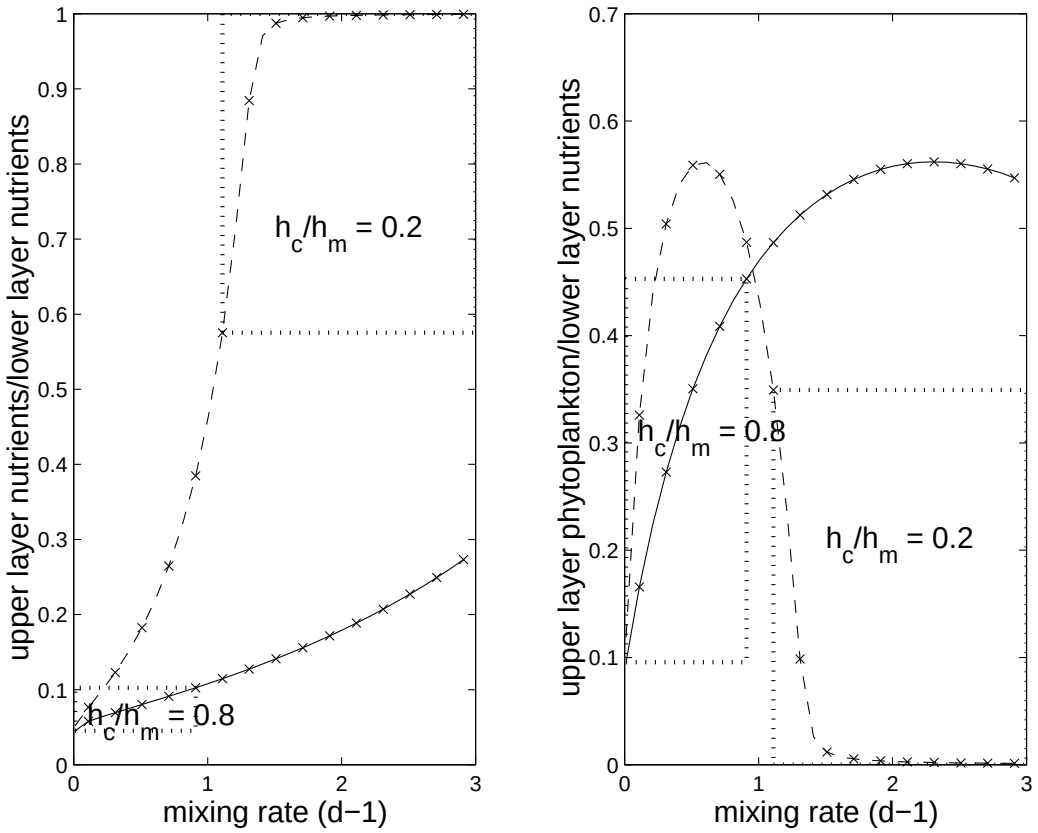

Figure 3: Two month means for upper layer (a) nutrients (b) phytoplankton concentrations from integration of Eqns 1 (normalized by lower layer nutrients) as a function of mixing rate, κ. Two different critical layer/mixed layer ratios: solid line for h_c/h_m=0.8 and dashed for h_c/h_m=0.2 are depicted. Crosses indicate individual experiments. Dotted boxes for the subtropical region, h_c/h_m=0.8, and subpolar region,region h_c/h_m=0.2, indicate expected values of mixing rates for those regions. The values for μ, N_o and β are 1.5 d^{-1}, 0.1 μM and 0.5 d^{-1}, respectively for these plots.

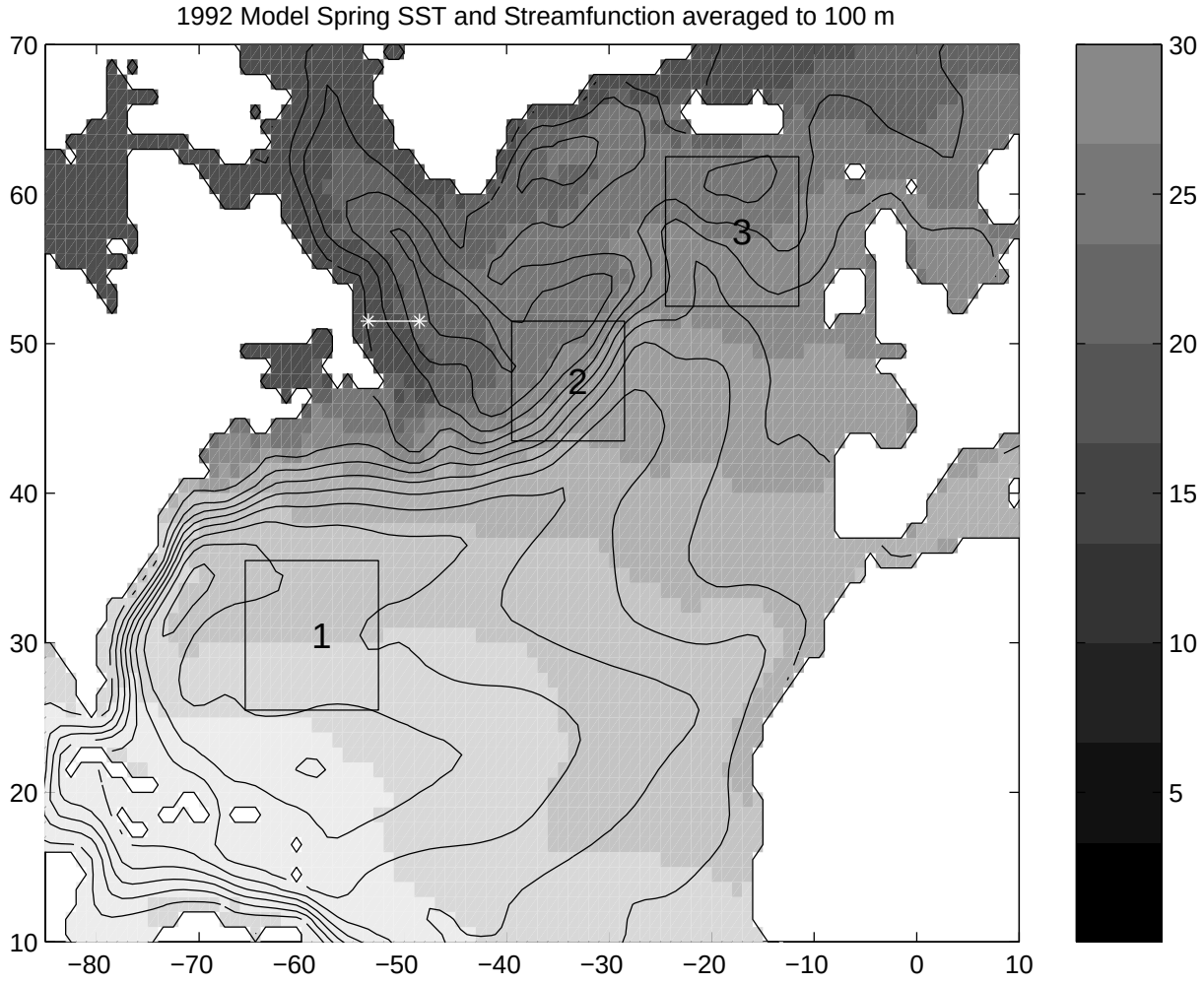

Figure 4: Model sea surface temperature (shading) and model geostrophic streamfunction averaged over 100m (contours) for the spring (March, April and May) of 1992. The boxes indicate: 1 = "subtropical region"; 2 = "intergyre region"; and 3 = "subpolar region". Also shown is the transect at 51^oN described in Section 4.2.2.

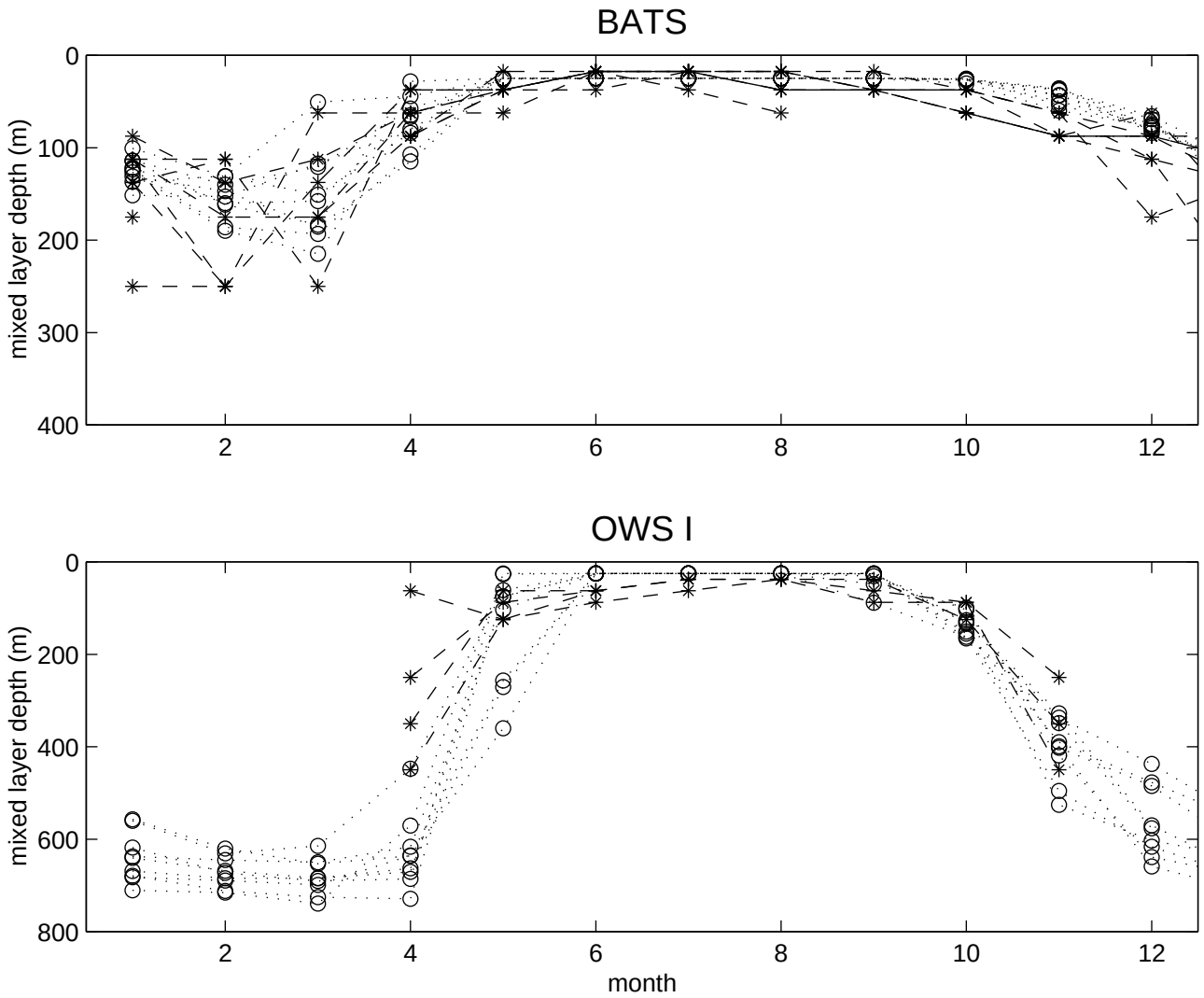

Figure 5: Model mixed layer depth (o) for "subtropical" (upper panel) and "subpolar" (lower panel) regions (see Fig. 4) compared to *in situ* (*) measurements at BATS (32^{o}N, 65^{o}W) and OWS "I" (59^{o}N, 19^{o}W). Mixed layer is defined as the depth where the difference between the temperature and the sea-surface temperature becomes greater than .5^{o}C. Dotted curves indicate each year of the model run, dashed curves indicate each year for which *in situ* data was available

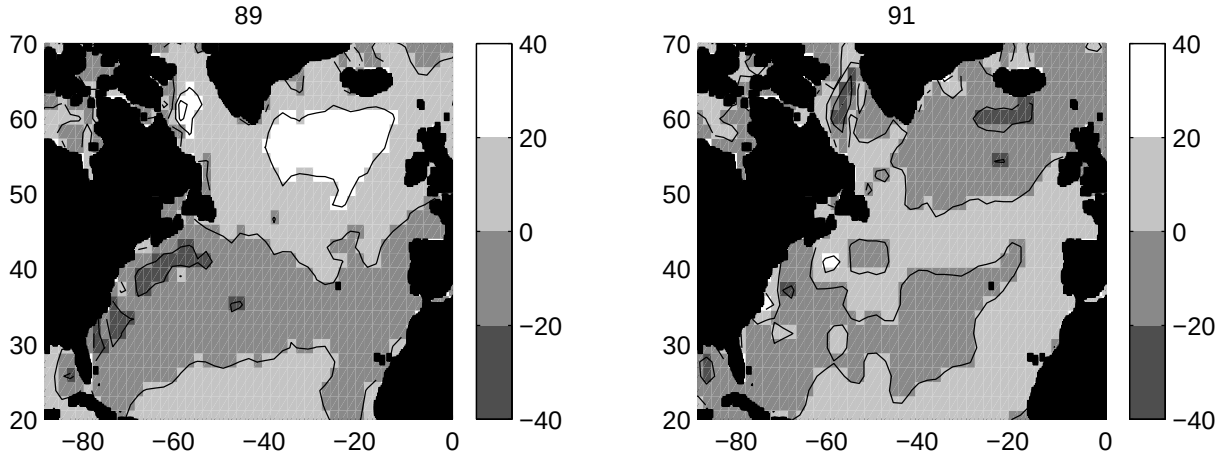

Figure 6: Anomaly of NCEP sensible heat flux (W/m^2) for winter/spring (January through June) 1989 and 1991 (mean taken over 1987 to 1995). Compare patterns of anomaly to those for model convection (Fig. 7).

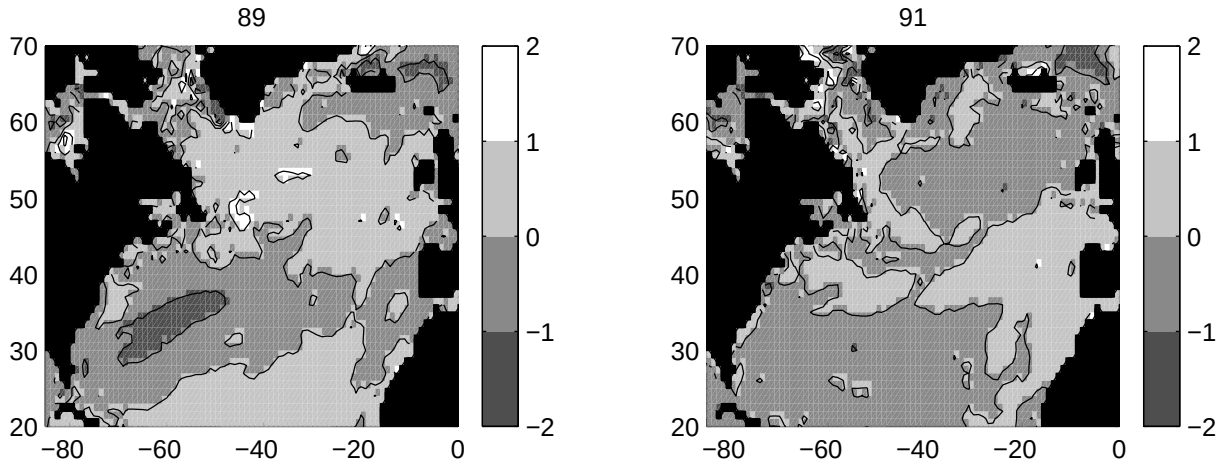

Figure 7: Anomaly of convective mixing rate (d^{-1}) over top 50 m for winter/spring (January through June) 1989 and 1991 (mean taken over 1987 to 1995).

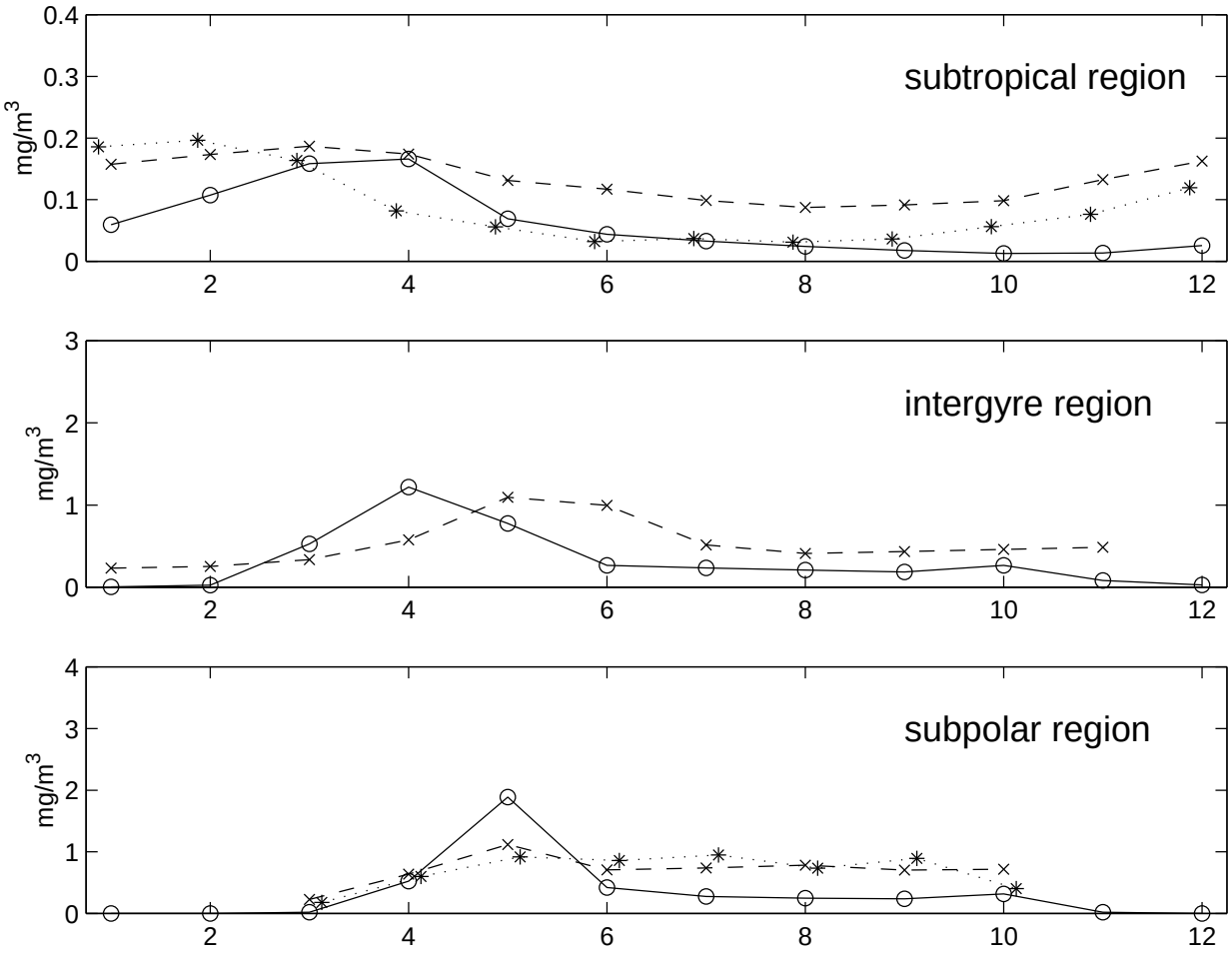

Figure 8: Chlorophyll (mg/m^3) in the regions shown in Fig. 4: (o) layer 1 of model averaged by month for the 9 year sequence; SeaWiFS monthly means for 1998 ($\times$); and *in situ* data (*) – BATS averaged for 1990 to 1996 in subtropical region and OWS "I" averaged for 1970 to 1975 in subpolar region.

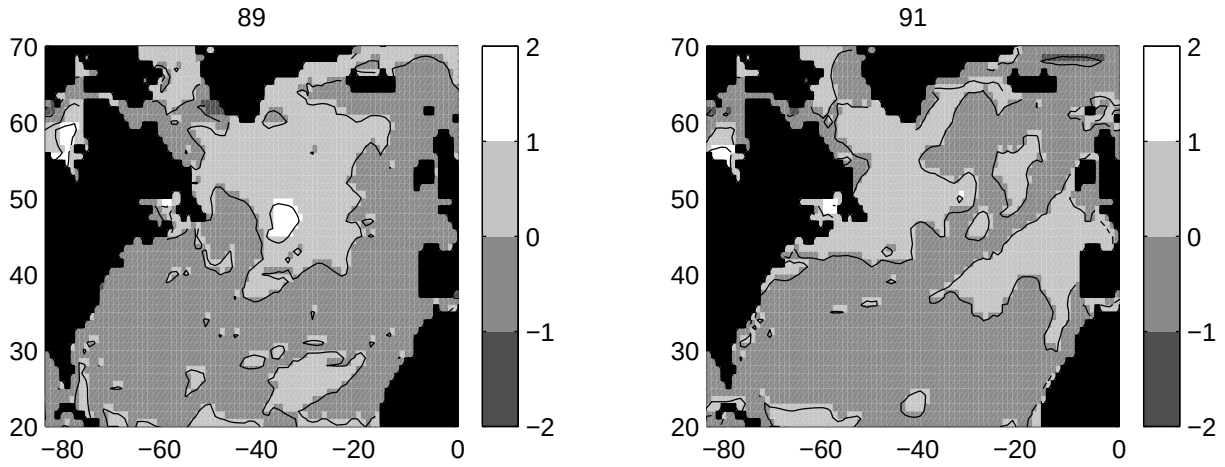

Figure 9: Anomaly of inorganic nitrogen concentration (μ M) over top 50 m for winter/spring (January through June) 1989 and 1991 (mean taken over 1987 to 1995).

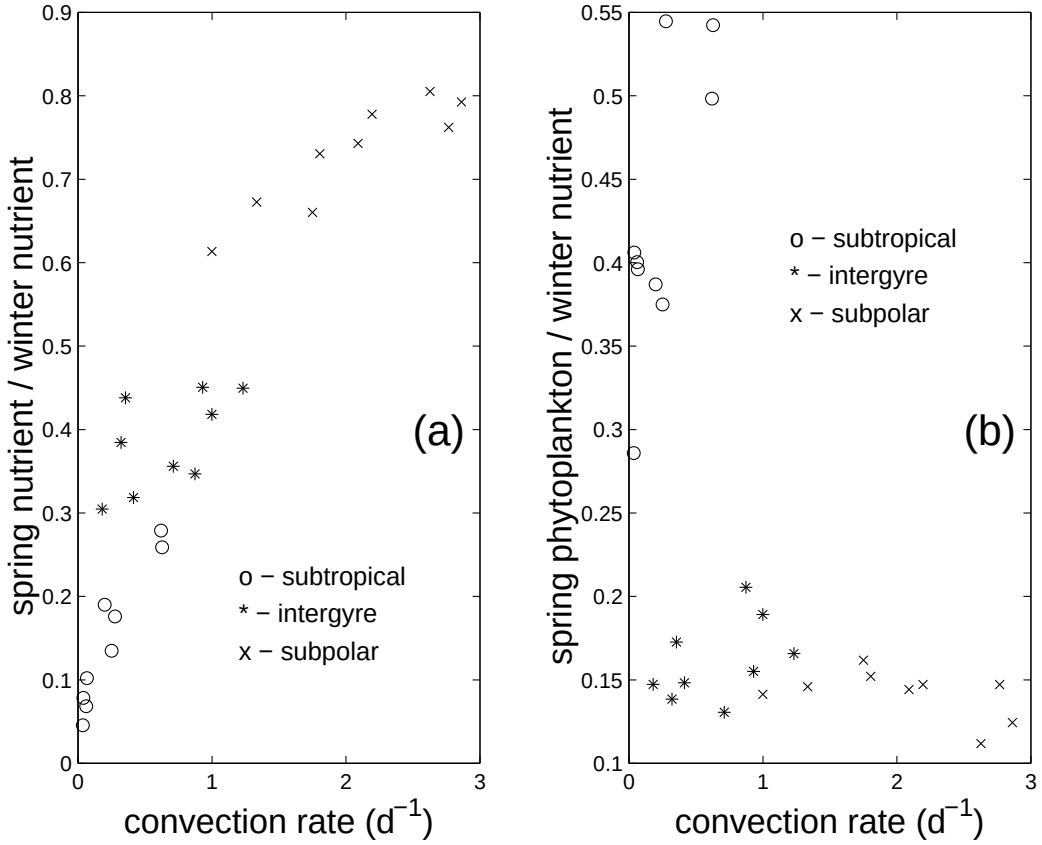

Figure 10: Mean upper 50 m (a) nutrient and (b) phytoplankton concentrations (normalized by mean 50-100 m of end of winter nutrients) during the spring (April and May) of the 9 years of the model results for the three regions shown in Fig. 4: o (subtropical); * (intergyre); $\times$ (subpolar). Convection rate is determined from the general circulation model's convective mixing statistics.

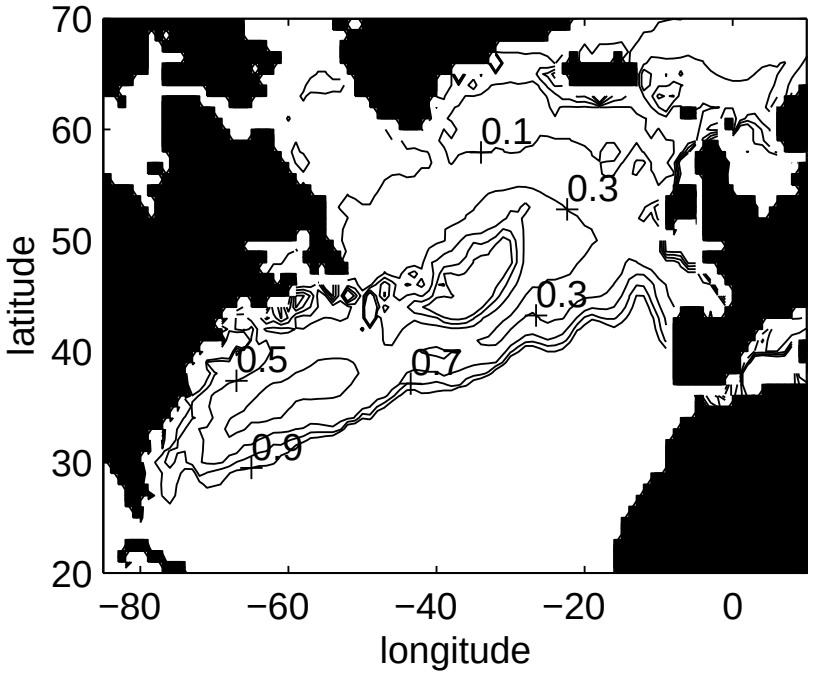

Figure 11: Model mean spring critical depth (April and May) and end of winter mixed layer depth (February and March) ratio (h_c/h_m).

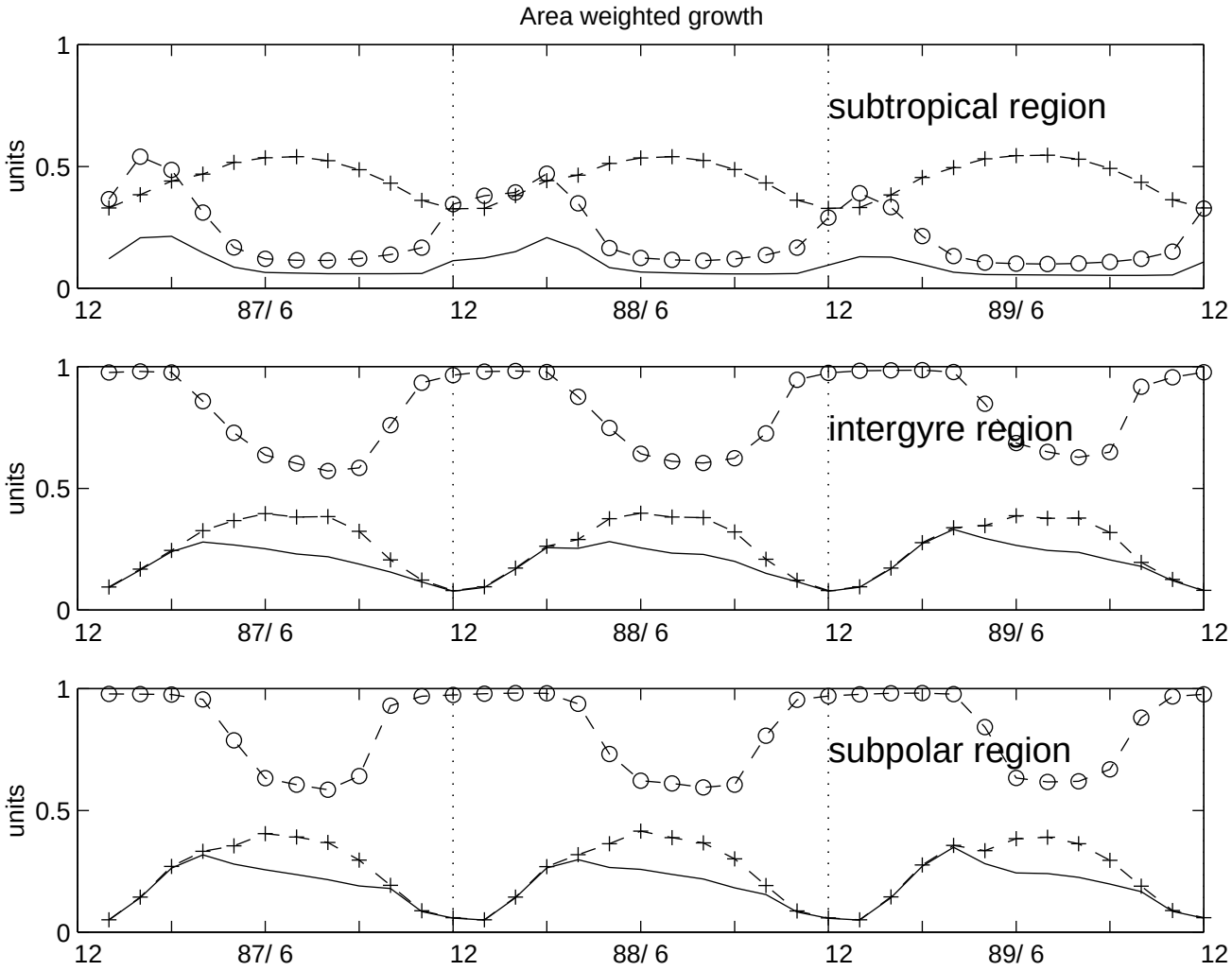

Figure 12: Model average for top 50 m for the three regions in Fig. 4: $\frac{N}{N+N_o}$ (o); $\frac{I}{I+I_o}$ (+); and $\frac{N}{N+N_o}\frac{I}{I+I_o}$ (solid line) (only years 1987 to 1989 are shown).

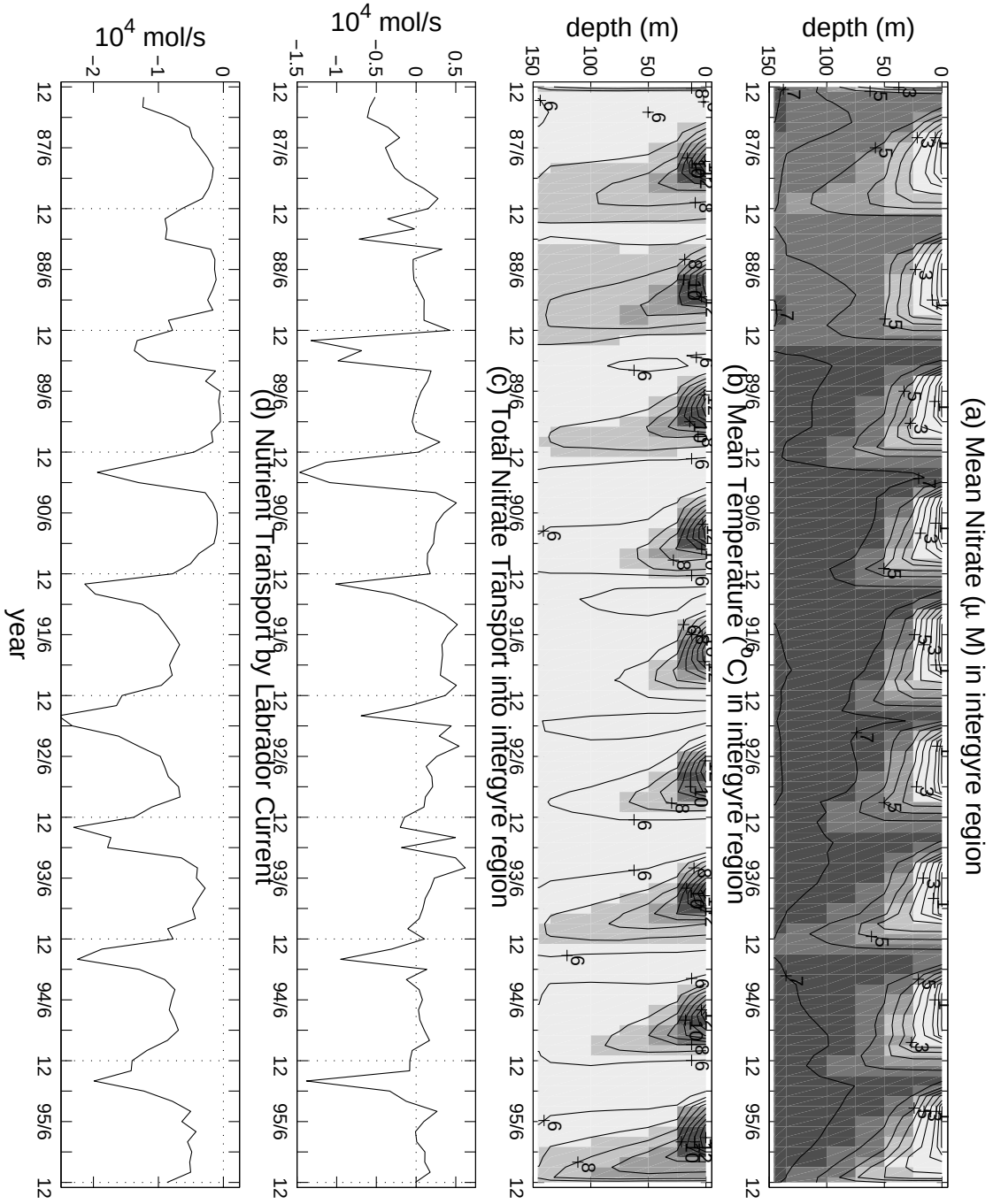

Figure 13: Profile of (a) model monthly mean inorganic nitrogen (μ M) concentrations and (b) temperature (^{o}C) in the intergyre region for the nine year sequence; (c) total transport of inorganic nitrogen into top 100 m of intergyre region (mol/s); (d) transport of inorganic nitrogen over top 100 m (mol/s) southward by Labrador Current at 51^{o}N (transect location shown in Fig. 4). Contours in (a) are .1, .5 and then every 1 μ M; contour interval in (b) is 1 ^{o}C.

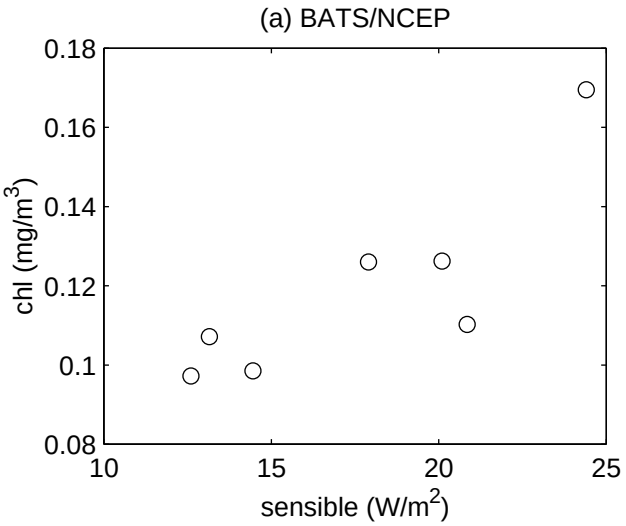

(a)

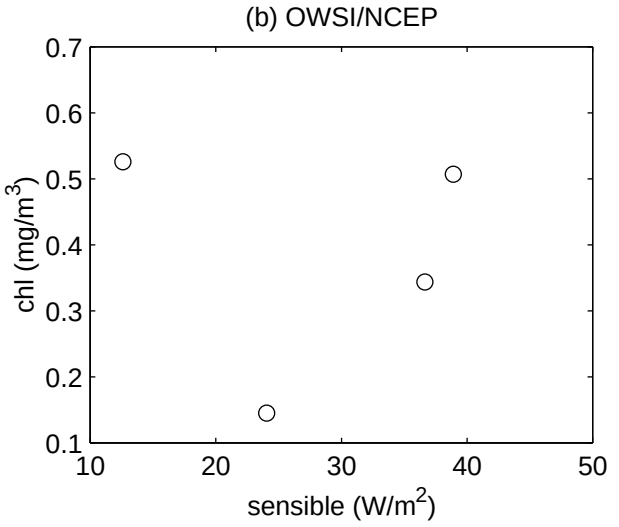

(b)

Figure 14: *In situ* surface Chlorophyll for each spring plotted against NCEP sensible heat flux for the $1^o \times 1^o$ region around (a) BATS (32^oN, 65^oW) for 1990 to 1996; (b) OWS "I" (59^oN, 19^oW) for 1970 to 1975 (when there is sufficient data).

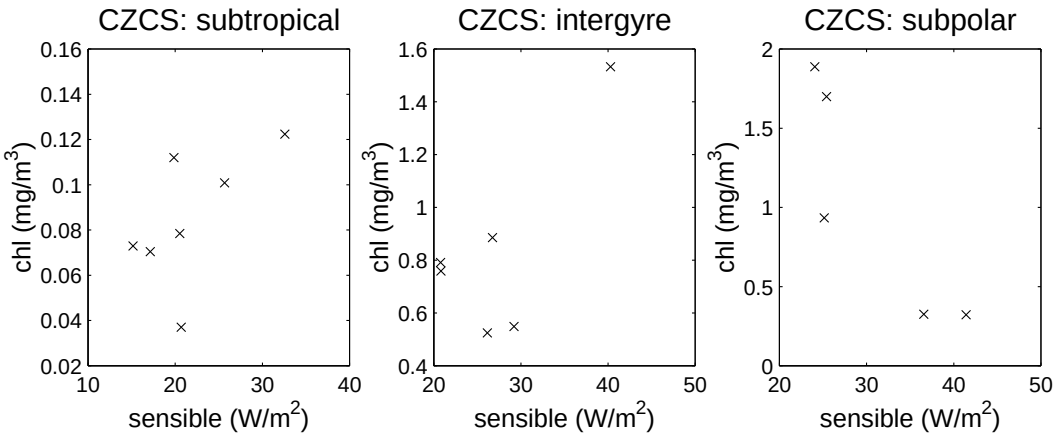

(a)

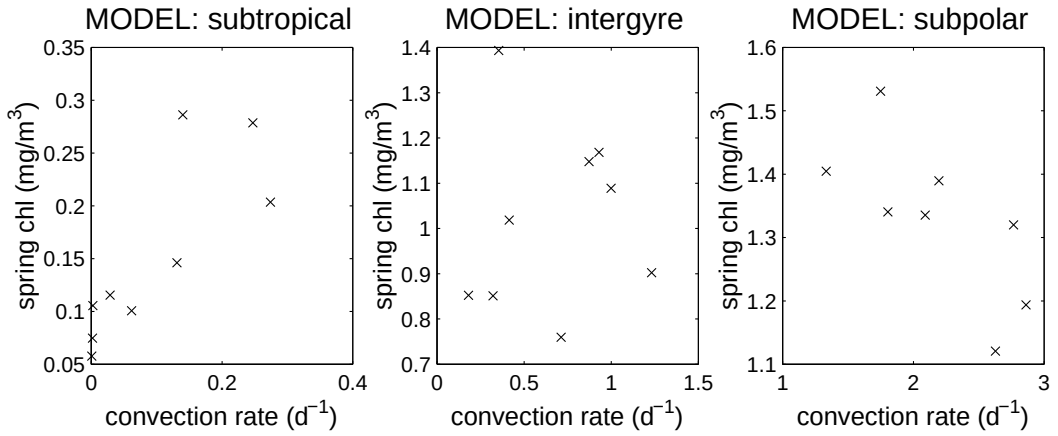

(b)

Figure 15: (a) Mean spring CZCS chlorophyll-a concentrations plotted against NCEP sensible heat flux for 1979 to 1986; and (b) Model spring mean chlorophyll concentration plotted against convective mixing rate, for the three regions shown in Fig. 4. Note that the model chlorophyll data is averaged to 50 m, so magnitudes should not be expected to match CZCS chlorophyll.